

NON-DESTRUCTIVE MEASUREMENT OF GREEN TILE BULK DENSITY BY X-RAY ABSORPTION

J.L. Amorós, C. Feliú, D. Llorens, V. Cantavella, A. Mezquita

Instituto de Tecnología Cerámica (ITC)
Asociación de Investigación de las Industrias Cerámicas
Universitat Jaume I. Castellón. Spain

ABSTRACT

The present study analyses the application of the X-ray absorption technique to the measurement of green tile bulk density. First, a theoretical study has been undertaken of X-ray absorption in ceramic materials in order to establish the influence of factors such as thickness, chemical composition and moisture content of the piece on X-ray absorption by the body, and to select the most appropriate working energy for the tests.

In the second phase of the study, a prototype has been developed (for which a patent has been applied) which enables analysing experimentally the influence of all the foregoing parameters on X-ray absorption, and determining the relations that allow calculating tile bulk density with high accuracy. The accuracy of the method has also been established.

1. INTRODUCTION

Bulk density is a key parameter in the manufacture of ceramic tiles. It influences the presence of calibres, departures from rectangularity, end porosity or drying processes, outgassing, pinholing and black core formation^[1-4]. At present this measurement is performed manually or semi-automatically by the mercury displacement method^[5]. Though this method is quite accurate, it entails the fundamental problem of using mercury, which is highly toxic^[6]. This problem has lately led to the search for other bulk density measurement methods, which differ essentially in the methods used for determining volume: they involve reconstructing the volume using laser telemetry or measuring the rise in air pressure produced by displacement of the test specimen volume to be measured, the specimen being protected by a membrane.

The use of X-rays offers multiple advantages compared with immersion in mercury: it enables obtaining a more detailed density distribution map, faster test speeds and no toxicity. The only precaution needed is a shield in the X-ray tube and detector zone to prevent X-ray leaks.

The objective of the study has been to demonstrate the technical feasibility of a bulk density measurement method based on X-ray absorption, which is capable of obtaining measurements with an error below 0.01 g/cm³, which would be a permissible value in industrial practice.

2. THEORETICAL ANALYSIS OF X-RADIATION ABSORPTION

All materials absorb X-radiation in a magnitude that depends on their chemical nature, thickness and bulk density^[7]. Therefore, if their chemical nature does not change and thickness is known, density can be derived from absorbed energy:

$$\frac{I'_{\lambda}}{I'_{\lambda 0}} = e^{-\mu_{\lambda} \rho h}$$

Equation 1

where:

$I'_{\lambda 0}$: flux density of incident radiation per unit wavelength (W/m³)

I'_{λ} : flux density of transmitted radiation per unit wavelength (W/m³)

μ_{λ} : X-ray absorption coefficient (m²/kg)

ρ : bulk density (kg/m³)

h : thickness of the piece (m)

Coefficient μ_{λ} depends on the X-ray wavelength and on the chemical nature of the material. If the relation $I'_{\lambda}/I'_{\lambda 0}$, μ_{λ} and h are known, equation 1 allows determining bulk density (ρ).

When X-radiation reaches the sensor, this generates a current I_{λ} that depends on I'_{λ} , on sensor efficiency at this wavelength (r_{λ}) and on a factor (k), which is a function of the characteristics of the photodiode, but not of the X-radiation wavelength:

$$I_{\lambda} = kr_{\lambda}I'_{\lambda}$$

Equation 2

The total signal generated by the photodiode is the sum of I_{λ} extended to all the wavelengths:

$$I = \int_{\lambda_0}^{\infty} I_{\lambda} d\lambda = k \int_{\lambda_0}^{\infty} r_{\lambda} I'_{\lambda_0} e^{-\mu_{\lambda} \rho h} d\lambda$$

Equation 3

where:

λ_0 : minimum wavelength (m)

I: current generated by the photodiode (A)

The value of λ_0 only depends on the X-ray tube voltage power supply, whereas the value of I'_{λ_0} depends, in addition, on the geometric and constructive characteristics of the tube, as well as on the distance between the tube and the sample, and on the distance between the X-ray beam axis and the point at which the intensity is being measured.

However, equation 3 is not very practical. If the radiation is 'almost' monochromatic, eq. 3 can be rewritten in a form similar to that of equation 1, though with mean values:

$$\frac{I}{I_0} = e^{-\mu \rho h}$$

Equation 4

where μ is the absorption coefficient. Note, however, that equation 4 is solely approximate.

From an intuitive point of view, μ can be interpreted as the 'opacity' of a material to the passage of X-rays of a given energy. The smaller μ is, the more transparent will the material be to radiation.

3. DESCRIPTION OF THE PROTOTYPE

In order to verify the applicability of the X-ray absorption method for the bulk density measurement, an assembly was designed whose operating scheme is depicted in figure 1.

In this assembly, the piece to be examined (1) is placed on a belt (7) for conveyance. An X-ray tube (2) generates a radiation that travels through the piece and is detected by a sensor (3). The sensor signal is amplified (4) and is transmitted to a computer (8).

To be able to calculate density from equation 4 it is necessary to know the thickness of the piece (h). For this, there are two telemeters (5 and 6), which send the signal to the computer (8).

The computer also commands the movements of the belt (7), which has a pair of x-y axes with two motors, though figure 1 only shows one of these. This enables scanning a whole piece. Finally, the assembly has lead shielding (9) to prevent any leakage of radiation emitted by the X-ray tube. Figure 2 presents a view of the prototype, installed in an enclosure (blue cabinet), which shields the operator from any radiation.

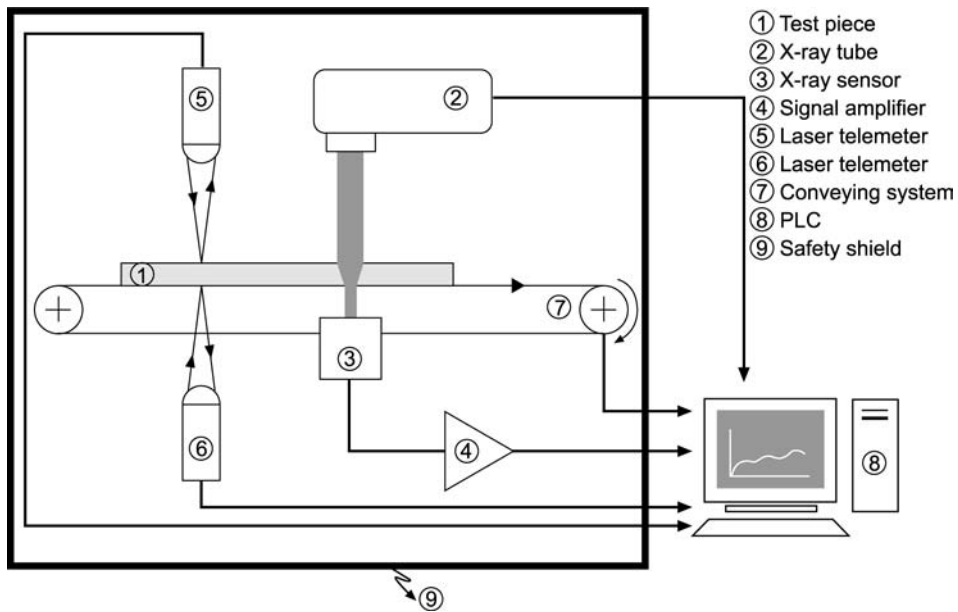


Figure 1. Operating scheme of the bulk density measurement assembly by X-radiation absorption.



Figure 2. Prototype for bulk density measurement by X-ray absorption.

4. MATERIALS AND EXPERIMENTAL PROCEDURE

4.1. MATERIALS AND TEST SPECIMEN PREPARATION

Test pieces of 15x15 cm were used, formed by uniaxial pressing of spray-dried powder of a standard red stoneware composition. The following variables were analysed:

- Bulk density
- Thickness of the pieces
- Moisture content of the pieces during testing
- Presence of ribs

In the three first cases, the pieces were ribless.

4.2. BULK DENSITY MEASUREMENT BY X-RAY ABSORPTION

After the pieces had been formed they were cut into parallelepiped test specimens of 3x15 cm; these were set in a holding frame, as shown in figure 3. After the test in the X-ray assembly, the specimens were cut up and the mean density of the top, centre and bottom zones were measured.

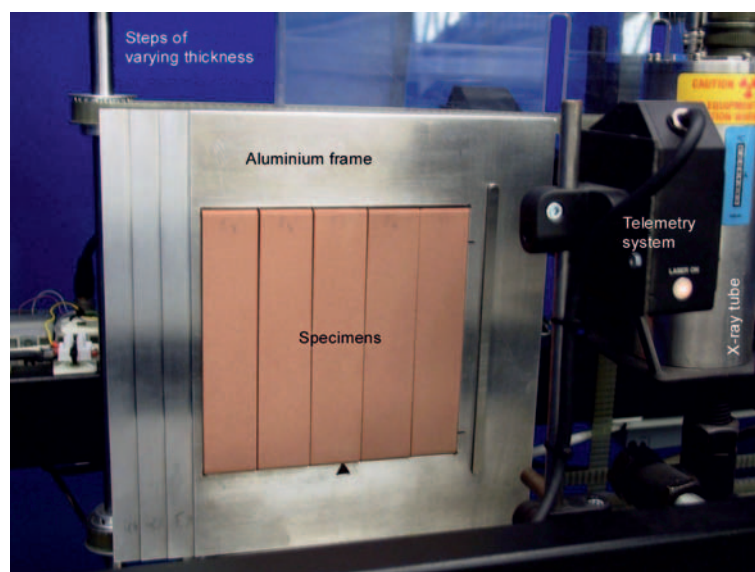


Figure 3. Arrangement of the test specimens in the aluminium frame for testing.

Data processing was performed with a program specially developed for this study. The software needed to solve several problems:

- *Thickness calibration.* Equation 4 indicates that if density is to be established with an error below 0.01 g/cm^3 , it is necessary to measure the thickness with an error below $50 \text{ }\mu\text{m}$. A thermal change of $10 \text{ }^\circ\text{C}$ could lead to an error of this magnitude. Therefore, it was necessary to perform automatic and periodic recalibration of the telemetry system. For this, the aluminium frame in which

the pieces were placed had a number of ‘steps’ of varying known thickness (figure 3), which were used by the software to perform the adjustments.

- *Correction of tube and sensor stability.* The high accuracy required by the method made it necessary to take into consideration the small fluctuations in X-ray intensity and in X-ray detection. The program has a procedure that corrects the deviations.
- *Obtainment of profiles and mean values of pre-selected regions.* This is important because the reference method (mercury displacement) used does not enable measuring point densities, but only mean values.
- *Map overlapping.* The assembly used does not allow measuring thickness and X-ray intensity, at a given moment, at the same point in the piece. There is a certain relative displacement between both types of sensors (see figure 1), which causes the thickness and X-ray intensity maps to be displaced relative to each other. This displacement needs to be taken into account in order to calculate density.

5. RESULTS AND DISCUSSION

5.1. INFLUENCE OF X-RADIATION ENERGY

The absorption coefficient μ can be calculated theoretically in a simple way. Its value only depends on the chemical composition (elementary analysis) with which, based on chemical analysis and knowledge of μ for the different elements, it is possible to calculate the value of μ for any composition using the additive formula:

$$\mu = \sum_i \omega_i \mu_i$$

Equation 5

where:

μ_i : atomic absorption coefficient of element E_i

ω_i : mass fraction of element E_i in the composition

The values of μ_i were obtained from the Photcoef© program Web site, though it is no longer available at this source. Subroutines in Fortran and C can be found at^[8], which allow making similar calculations.

Figure 4 shows the X-ray absorption coefficient of a red stoneware composition, for different energies (from 0.1 to 100 keV). It can be observed that μ decreases very quickly as radiation energy increases. X-rays of higher energies will be more penetrating, and will be able to travel through greater piece thicknesses. The discontinuities that appear at given energies are characteristic of the electronic transitions of the elements that make up the material and, hence, depend on the composition.

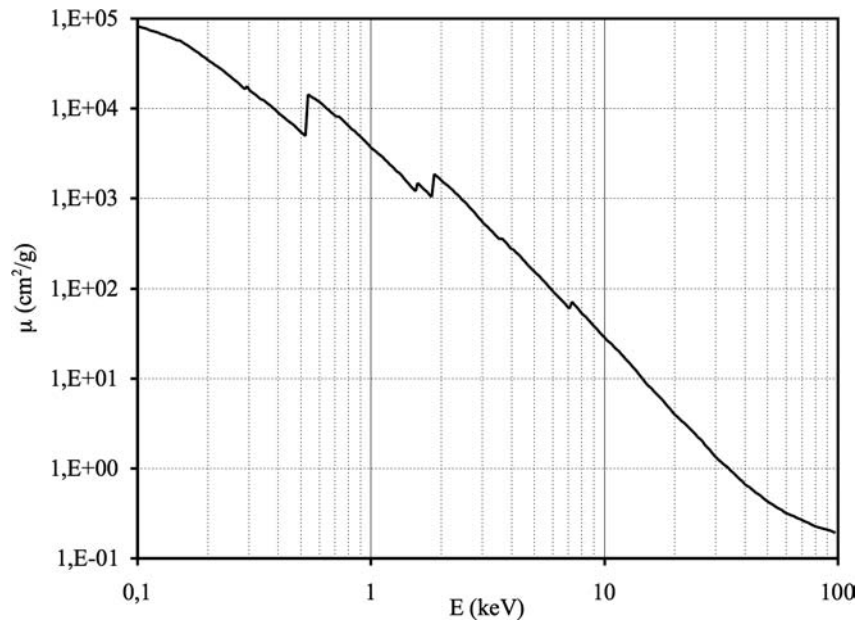


Figure 4. Theoretical estimation of the absorption coefficient μ as a function of X-radiation energy.

Equation 5 enables establishing how μ varies with composition and, therefore, also with moisture. The results obtained show that the type of material (red stoneware, white stoneware, etc.) has a sufficiently important influence on μ to make it necessary to use different calibrations for different materials.

Moisture content has a much less important effect, and is strongly dependent on X-ray energy. A 3% variation in moisture leads to a change of 5% in μ at 1 keV, of 1% at 10 keV and of 2.5% at 50 keV.

5.2. DETERMINATION OF THE RELATION BETWEEN BULK DENSITY AND TRANSMITTED X-RADIATION INTENSITY

5.2.1. Tests with specimens of constant thickness and variable bulk density

From equation 4 it can be inferred that the relation between $\ln I$ and ρh should be a straight line, whose slope would enable determining μ . This plot is presented in figure 5 for different X-ray tube voltages and electric current intensities. It shows that in the four tested conditions a straight line is obtained. However, it was verified that at high thicknesses (above 8.5 mm) it was better to work at a voltage of 45 kV.

A further feature of figure 5 is the great sensitivity of X-ray intensity (I) to variations in tube voltage or electric current. In practice this means that control and stability of the tube need to be very accurate.

We analysed five test specimens of 3x15 cm of different density with the selected voltage and intensity values. These specimens were all about 8 mm thick. Three regions were distinguished in each test specimen: bottom (I), centre (C) and top (S). Table 1 (test E1) lists the experimentally measured density values (column ρ_{exp}), as well as the values calculated from the fit of eq. 4 and the error (difference between the result of the fit and the experimental value). It can be observed that the fit is very good, with a maximum error of 0.008 g/cm³ and a mean absolute error of 0.003 g/cm³.

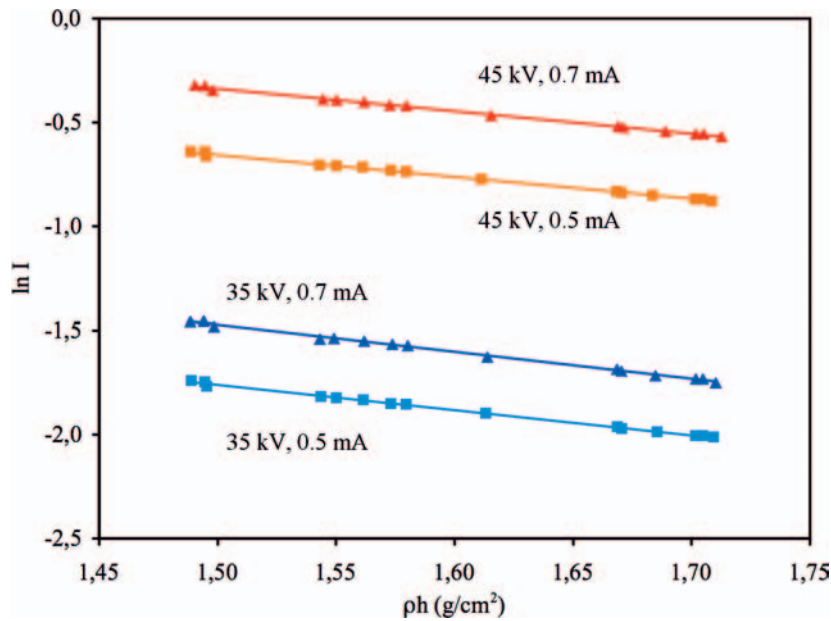


Figure 5. Plot of $\ln I$ versus surface density (ρh) for different X-ray tube voltages and current intensities.

		TEST E1			TEST E2				
PIECE	POS	ρ exp (g/cm ³)	ρ fit (g/cm ³)	$\Delta\rho$ fit (g/cm ³)	ρ exp (g/cm ³)	ρ estima (g/cm ³)	$\Delta\rho$ estima (g/cm ³)	ρ correc (g/cm ³)	$\Delta\rho$ correc (g/cm ³)
P1	I	1.927	1.923	-0.004	1.911	1.897	-0.014	1.905	-0.006
	C	1.926	1.924	-0.002	1.915	1.909	-0.006	1.917	0.002
	S	1.920	1.917	-0.003	1.898	1.891	-0.007	1.903	0.005
P2	I	1.974	1.976	0.002	1.979	1.974	-0.005	1.980	0.001
	C	2.004	2.002	-0.002	1.990	1.983	-0.007	1.992	0.002
	S	1.990	1.992	0.002	1.986	1.976	-0.010	1.991	0.005
P3	I	2.030	2.032	0.002	2.047	2.041	-0.006	2.047	-0.000
	C	2.041	2.049	0.008	2.047	2.048	0.001	2.058	0.011
	S	2.047	2.051	0.004	2.042	2.033	-0.009	2.049	0.007
P4	I	2.110	2.116	0.006	2.116	2.106	-0.010	2.114	-0.002
	C	2.108	2.109	0.001	2.092	2.082	-0.010	2.093	0.001
	S	2.104	2.107	0.003	2.084	2.068	-0.016	2.085	0.001
P5	I	2.164	2.159	-0.005	2.159	2.154	-0.005	2.161	0.002
	C	2.167	2.163	-0.004	2.172	2.159	-0.013	2.172	-0.000
	S	2.147	2.143	-0.004	2.162	2.150	-0.012	2.168	0.006
			Mean $ \Delta\rho $ fit	0.003		Mean $ \Delta\rho $ estima	0.009	Mean $ \Delta\rho $ correc	0.003

Table 1. Experimental and calculated density values using the X-ray absorption method.

To validate the method, a further test (E2) was conducted in which new pieces were analysed using the calibration obtained in test E1. Table 1 details the experimental density obtained in this test, as well as the estimated density (column ρ estima) from the E1 calibration. In this case, the errors are found to be more important and, although the mean absolute error lies within the target specification, there are individual values which exceed this, with maximum errors of 0.016 g/cm³.

These results are not permissible, in particular, since they have been obtained in pilot plant conditions, while industrial conditions would probably be worse.

The causes of these high errors are to be sought in the possible variations of the X-ray tube, in the chain of measurement or in ambient factors (such as variations in temperature). In an attempt to account for these factors it was proposed that the parameters of eq. 4 could change slightly, and not be exactly the same when the calibration standards were analysed as when the problem pieces were analysed:

Parameters during calibration

$$I = I_0 e^{-\mu \rho h}$$

Equation 6

Parameters during analysis of the problem pieces:

$$I = I_0^* e^{-\mu^* \rho h} = \phi_0 I_0 e^{-\phi_1 \mu \rho h}$$

Equation 7

Thus, ϕ_0 and ϕ_1 would be equal to 1 during the calibration and would have a value different from 1 during analysis of the problem pieces. The problem, however, is that the value of these parameters needs to be known. To determine ϕ_0 and ϕ_1 the X-ray signal that crossed the aluminium frame containing the test specimen was analysed. Applying equation 4 to the aluminium frame gives:

Parameters during calibration

$$I_R = I_{0R} e^{-\mu_R \rho h}$$

Equation 8

Parameters during analysis of the problem pieces:

$$I_R = I_{0R}^* e^{-\mu_R^* \rho h} = \phi_0 I_{0R} e^{-\phi_1 \mu_R \rho h}$$

Equation 9

I_{0R} , μ_R , I_{0R}^* and μ_R^* can be determined experimentally. Therefore, the dimensionless factors ϕ_0 and ϕ_1 in equation 9 are known. As a working hypothesis, it was proposed to set these factors equal to those in equation 7.

Table 1 (column ρ correc) shows the corrected density values using the procedure described previously. It is observed that, with this new method, the errors have been considerably reduced: there is now a mean absolute error of 0.003 g/cm³ and a maximum error of 0.011 g/cm³, which lies within the target specifications.

5.2.2. Tests with specimens of variable thickness and constant bulk density

Equation 4 includes the effect of thickness. However, the tests shown in table 1 had all been performed with pieces of the same thickness. The influence of this parameter had, therefore, not been verified experimentally.

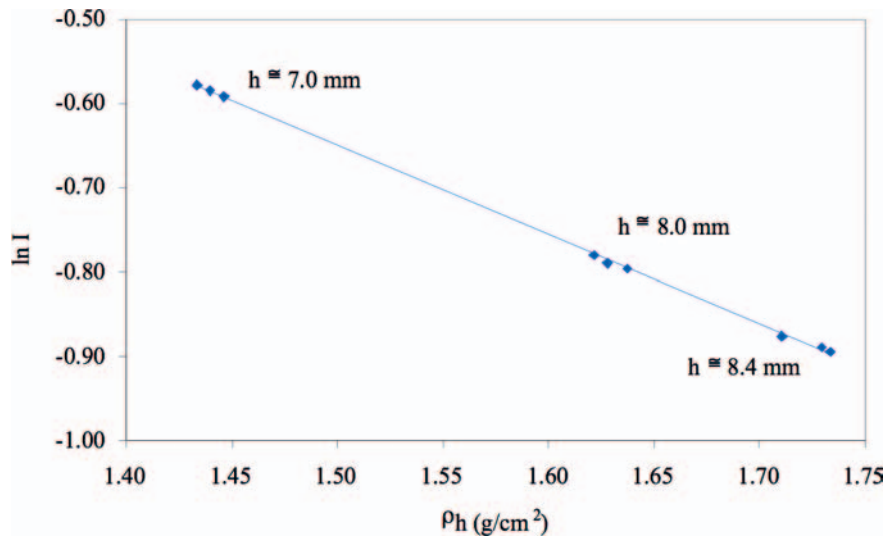


Figure 6. Plot of $\ln I$ versus surface density (ρh) for test specimens of different thickness and practically the same density.

Figure 6 plots the logarithm of X-ray intensity as a function of surface density (ρh) for pieces of different thickness. The results also fit a straight line. However, for the X-ray absorption method to be applicable, the foregoing linearity is not sufficient; it is necessary, from a preliminary calibration, that it should be possible to predict the density.

Table 2 sets out experimental thickness and density values of the tested pieces, together with the result of the application of the calibration obtained with test E1 (column ρ estima). It can be observed that the error is relatively large. With a view to reducing the error, equation 7 was applied, which uses correction parameters ϕ_0 and ϕ_1 . The results obtained are also given in table 2 (column ρ correc). In this second case the errors are much smaller and are perfectly admissible.

		TEST E3					
PIECE	POS	h (mm)	ρ exp (g/cm ³)	ρ estima (g/cm ³)	$\Delta\rho$ estima (g/cm ³)	ρ correc (g/cm ³)	$\Delta\rho$ correc (g/cm ³)
P1	I	7.07	2.045	2.027	-0.018	2.040	-0.005
	C	6.98	2.062	2.044	-0.018	2.058	-0.004
	S	6.97	2.056	2.040	-0.016	2.054	-0.002
P2	I	8.01	2.032	2.022	-0.010	2.035	0.003
	C	7.99	2.029	2.016	-0.013	2.031	0.002
	S	8.04	2.036	2.020	-0.016	2.035	-0.001
P3	I	8.48	2.044	2.026	-0.018	2.040	-0.004
	C	8.39	2.061	2.041	-0.020	2.057	-0.004
	S	8.38	2.041	2.025	-0.016	2.040	-0.001
				Mean $ \Delta\rho $ estima	0.016	Mean $ \Delta\rho $ correc	0.003

Table 2. Experimental and calculated density values using the X-ray absorption method.

5.2.3. Effect of test specimen moisture content

In industrial practice, tile density is measured at the press exit, in conditions in which the tiles are moist. The moisture content can vary in time, either as a result of variations in spray-dried powder moisture content, or because the tiles dry slightly during the time that elapses from collection to testing.

Note, however, that the parameter to be controlled is dry and not wet tile density. In many companies, for the sake of speed, wet density is determined, assuming this is equivalent or proportional to dry density. But this is only true if the moisture content remains constant.

In any case, it is important to quantify the effect that moisture content and its variations have on dry density by the X-ray method. Basically, the presence of water in the tiles modifies the values of ρ and μ in eq. 4. Eq. 5 enables establishing the influence of moisture content, as indicated previously, from:

$$\varepsilon(\rho) = \rho_0 - \rho = \frac{\mu_w}{\mu_s} \rho X$$

Equation 10

where:

- $\varepsilon(\rho)$: error in density (kg/m^3)
- ρ_0 : dry density calculated from X-ray absorption, without considering moisture (kg/m^3)
- ρ : dry density calculated from X-ray absorption, considering moisture (kg/m^3)
- μ_w : coefficient of X-ray absorption of the water (m^2/kg)
- μ_s : coefficient of X-ray absorption of the dry solid (m^2/kg)
- X : moisture content on a dry basis ($\text{kg water}/\text{kg dry solid}$)

Therefore, the error in the determination of ρ is directly proportional, theoretically, to moisture content. Fortunately, the value of μ_w is smaller than that of μ_s , so that the effect of moisture is likely to be small.

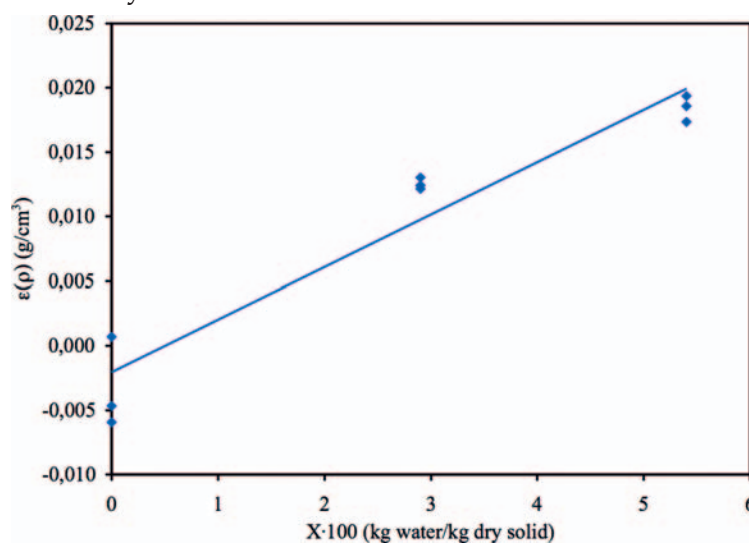


Figure 7. Effect of moisture content on error in the dry bulk density measurement.

In order to verify experimentally the role of moisture, specimens of the same density and thickness were tested, in which only moisture content varied. Figure 7 presents the results obtained, in the form of a plot of the error in density versus moisture.

It can be observed that the effect of moisture hardly modifies the density value. The slope of the straight line is $0.0041 \text{ (g/cm}^3\text{)/(kg water/kg dry solid}\cdot 100\text{)}$, which means that a variation of 1% in moisture would produce an error of 0.0041 g/cm^3 in the density estimated by this method.

In practice, making a calibration with dry pieces (similar to that effected in test E1), and using an approximate value for moisture (with an absolute error of 2%) would suffice to allow the X-ray absorption method to obtain the bulk density with sufficient accuracy (error below 0.01 g/cm^3).

5.3. TESTS ON INDUSTRIAL TILES

Industrial tiles have ribs: this means they have areas of variable thickness and density. To study the effect of a rib on the bulk density estimation by the X-ray absorption method, two tiles with ribs of different depth were prepared (0.74 and 1.41 mm, respectively).

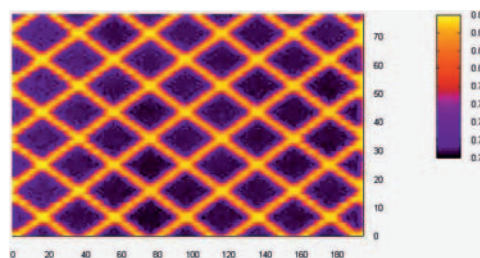


Figure 8. Map of thickness (scale in cm)

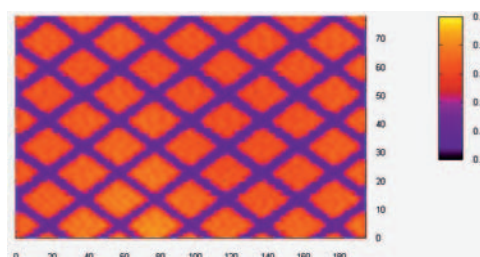


Figure 9. Map of X-ray intensity (scale in V)

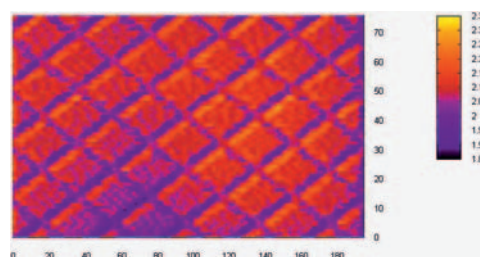


Figure 10. Map of density (scale in g/cm^3)

Figure 8 depicts the map of thickness measured by the laser telemeters, in which the thickness pattern produced by the rib can clearly be observed. Figure 9 presents the map of X-ray intensity, which shows that the intensity is less at those points where the rib is found, i.e. there is greater absorption. However, this does not mean that the density is greater, as will be shown below.

The thickness and X-ray intensity maps were then combined, taking into account the relative displacement existing between these, which yielded the density map using equation 9 and the calibration performed in test E1. The results are presented in figure 10. It shows that the ribs have a slightly smaller density than the rest of the tile.

In order to verify the results of figure 10 the tiles were cut up into 9 test pieces and the experimental density, determined by the mercury displacement method, was compared with the theoretical density calculated from the mean density that each test piece would have according to the map in figure 10.

TEST E4 - TILE P1				TEST E4 - TILE P2			
RIB DEPTH: 0.74 mm				RIB DEPTH: 1.41 mm			
POS	ρ_{exp} (g/cm ³)	ρ_{correc} (g/cm ³)	$\Delta\rho_{\text{correc}}$ (g/cm ³)	POS	ρ_{exp} (g/cm ³)	ρ_{correc} (g/cm ³)	$\Delta\rho_{\text{correc}}$ (g/cm ³)
I-De	2.062	2.060	-0.002	I-De	2.074	2.072	-0.002
C-De	2.071	2.070	-0.001	C-De	2.095	2.095	0.000
S-De	2.071	2.072	0.001	S-De	2.084	2.089	0.005
I-Ce	2.056	2.057	0.001	I-Ce	2.050	2.050	0.000
C-Ce	2.063	2.063	0.000	C-Ce	2.088	2.092	0.004
S-Ce	2.063	2.064	0.001	S-Ce	2.093	2.098	0.005
I-Iz	2.051	2.053	0.002	I-Iz	2.045	2.041	-0.004
C-Iz	2.067	2.067	0.000	C-Iz	2.076	2.075	-0.001
S-Iz	2.074	2.075	0.001	S-Iz	2.078	2.083	0.005
		Mean $ \Delta\rho _{\text{correc}}$	0.001			Mean $ \Delta\rho _{\text{correc}}$	0.003

Table 3. Experimental and calculated density values using the X-ray absorption method.

Table 3 sets out the density values for the nine test pieces of each tile. The test pieces have been arranged in rows (bottom (I), centre (C) and top (S)) and columns (right (De), centre (Ce) and left (Iz)). The results confirm that the X-ray absorption method enables estimating bulk density with great accuracy.

6. CONCLUSIONS

- A prototype and a computer program have been developed that enable obtaining a map of tile thickness, of the intensity of the X-rays that travel through the tile and of bulk density. These maps provide significant information, such as: differences in density or thickness between points of the same tile, and mean value of 'absolute' bulk density in different regions of the tile.
- The prototype developed has demonstrated that the X-ray absorption method allows measuring the bulk density of green ceramic tiles with an absolute error below 0.01 g/cm³.

- If high accuracy is to be obtained, it is necessary to correct the fluctuations in the system X-ray tube–detector–telemeters–chain of measurement. This can be done in a simple way by using a reference material that is tested whenever a calibration is made, or when the problem pieces are measured.
- Moisture content does not significantly affect the value of dry density determined by the X-ray absorption method.
- It is necessary to measure thickness with high accuracy and without contact. This can be done by means of appropriate laser telemeters.
- It has been verified that the method is applicable to tiles of different thickness, with the same choice of X-ray tube voltage and current intensity values. It is also applicable when the tile has variations in thickness, as in the case of ribs.

REFERENCES

- [1] AMORÓS, J.L.. *Pastas cerámicas para pavimentos de monococción: Influencia de las variables de prensado sobre las propiedades de la pieza en crudo y sobre su comportamiento durante el prensado y la cocción*. Valencia: Universidad, 1987, p. 61. [Ph.D. dissertation]
- [2] AMORÓS, J.L. et al. La operación de prensado en la fabricación de pavimento por monococción: I Influencia de la naturaleza del polvo de prensas sobre las propiedades de la pieza en crudo. *Bol. Soc. Esp. Ceram. Vidrio*, 27(5), 273-282, 1988.
- [3] AMORÓS, J.L. et al. La operación de prensado de pavimentos por monococción: II Influencia de la naturaleza del polvo de prensas sobre las propiedades de la pieza en cocido. *Bol. Soc. Esp. Ceram. Vidrio*, 29(3), 151-158, 1990.
- [4] ESCARDINO, A.; AMORÓS, J.L.; BELTRÁN, V.. Cinética de la oxidación de la materia orgánica en productos cerámicos prensados. In: *I Congreso Iberoamericano de Cerámica, Vidrio y Refractarios*. Arganda del Rey: Sociedad Española de Cerámica y Vidrio, 1983. pp. 317-329.
- [5] ENRIQUE, J.E. et al. *Controles de fabricación de pavimentos y revestimientos cerámicos*. Castellón: AICE, 1989, pp. 317-329.
- [6] MATERO, M.D. et al. Revisión sobre el mercurio como metal contaminante. *Química Analítica*, 7(2), 117-143, 1988.
- [7] BERTIN, E.P. *Principles and practice of x-ray spectrometric analysis*. New York: Plenum Press, 1984, pp. 51-55.
- [8] *X-ray absorption cross sections (McMaster) tables*. [on-line] [Consulted: 07/09/2005] <<http://ixs.csrii.iit.edu/database/programs/mcmaster.html>>